

Rapid communication

# Crystal structure of the pyrochlore oxide superconductor $\text{KOs}_2\text{O}_6$

Jun-Ichi Yamaura\*, Shigeki Yonezawa, Yuji Muraoka, Zenji Hiroi

*Institute for Solid State Physics, The University of Tokyo, Kashiwa, Chiba 277-8581, Japan*

Received 10 September 2005; received in revised form 20 October 2005; accepted 20 October 2005

Available online 2 December 2005

## Abstract

We report the single-crystal X-ray analysis of the structure of the pyrochlore oxide superconductor  $\text{KOs}_2\text{O}_6$ . The structure was identified as the  $\beta$ -pyrochlore structure with space group  $Fd\bar{3}m$  and lattice constant  $a = 10.089(2) \text{ \AA}$  at 300 K: the K atom is located at the  $8b$  site, not at the  $16d$  site as in conventional pyrochlore oxides. We found an anomalously large atomic displacement parameter  $U_{\text{iso}} = 0.0735(8) \text{ \AA}^2$  at 300 K for the K cation, which suggests that the K cation weakly bound to an oversized  $\text{Os}_{12}\text{O}_{18}$  cage exhibits intensive rattling, as recently observed for clathrate compounds. The rattling of A cations is a common feature in the series of  $\beta$ -pyrochlore oxide superconductors  $\text{AOs}_2\text{O}_6$  ( $A = \text{Cs, Rb and K}$ ), and is greatest for the smallest K cation.

© 2005 Elsevier Inc. All rights reserved.

PACS: 64.10.Nz; 63.20.Pw; 63.20.Ry; 74.70.Dd

Keywords: Pyrochlore oxides; Superconductor; Crystal structure; Rattling

## 1. Introduction

Pyrochlore oxides exhibit many fascinating phenomena, such as metal–insulator transition, superconductivity, magnetic frustration, colossal magnetoresistance, and ferroelectrics [1]. The first pyrochlore oxide superconductor  $\text{Cd}_2\text{Re}_2\text{O}_7$  with  $T_c = 1.0 \text{ K}$  was found in 2001 and is now believed to be a conventional BCS-type superconductor [2]. Recently, a new family of pyrochlore oxide superconductors  $\text{AOs}_2\text{O}_6$  was discovered, with  $T_c = 3.3, 6.3$  and  $9.6 \text{ K}$  for  $A = \text{Cs, Rb and K}$ , respectively [3–6]. Several experimental results for  $\text{KOs}_2\text{O}_6$  with the highest  $T_c$  have indicated unconventional features of superconductivity; the absence of a coherence peak in NMR experiments [7], a large upper critical field  $H_{c2} \sim 38 \text{ T}$  [8], and an anisotropic order parameter from muon spin rotation ( $\mu\text{SR}$ ) experiments [9]. In contrast, experimental results for  $A = \text{Cs and Rb}$  have indicated rather conventional features, although the mechanism of superconductivity is likely the same among the three compounds [6,7].

In ordinary pyrochlore oxides with the chemical formula  $\text{A}_2\text{B}_2\text{O}_6\text{O}'$ , the A cation, which is a large, rare-earth alkali metal, alkaline earth metal or post-transition metal cation, lies in a distorted ( $6\text{O} + 2\text{O}'$ ) coordination, while the B cation, which is a small transition metal cation, forms a slightly distorted  $\text{BO}_6$  octahedron. In the space group  $Fd\bar{3}m$  with the origin chosen at the B site, the A, B, O and O' atoms occupy the  $16d, 16c, 48f$  and  $8b$  Wyckoff positions, respectively. The crystal structure of  $\text{AOs}_2\text{O}_6$  was preliminarily reported to be the  $\beta$ -pyrochlore structure, in which the alkali metal cation A moves from the  $16d$  site to the  $8b$  site, replacing the O' atom of the conventional ( $\alpha$ -) pyrochlore oxides, while the B(Os)–O network remains intact [3–6]. A similar structure is observed in so-called defect pyrochlore oxides. For instance, in  $\text{ANbWO}_6$  with  $A = \text{Cs, Rb and K}$ , large Cs and Rb atoms occupy the  $8b$  site, while the smaller K atom lies at the  $32e$  site away from the  $8b$  site [10]. Moreover, it is known that in  $\text{KNbWO}_6$  a water molecule can be intercalated near the  $8b$  site, pushing a K atom towards the  $16d$  site. Structural refinements have been carried out for  $A = \text{Cs and Rb}$  by Rietveld analysis using synchrotron X-ray powder diffraction [11]. The lattice constants at room temperature are  $10.15250(4)$  and

\*Corresponding author. Fax: +81 47136 3461.

E-mail address: [jyamaura@issp.u-tokyo.ac.jp](mailto: jyamaura@issp.u-tokyo.ac.jp) (J.-I. Yamaura).

10.11760(4) Å, and the atomic coordinates  $x$  of the 48*f* oxygen are 0.3146(3) and 0.3180(3) for CsOs<sub>2</sub>O<sub>6</sub> and RbOs<sub>2</sub>O<sub>6</sub>, respectively. Remarkably large atomic displacement parameters are observed for alkali metal atoms:  $U_{\text{iso}} = 0.025 \text{ \AA}^2$  and  $U_{\text{iso}} = 0.043 \text{ \AA}^2$  for Cs and Rb, respectively, which are much greater than  $U_{\text{iso}} \sim 0.009 \text{ \AA}^2$  for Os atoms. On the other hand, detailed structural analysis for KOs<sub>2</sub>O<sub>6</sub> has not yet been reported because of difficulty in obtaining a single-phase polycrystalline sample and because of the hygroscopic nature of the powdered sample. In this paper, we report the first X-ray structural analysis of KOs<sub>2</sub>O<sub>6</sub> using a fresh single crystal.

## 2. Experimental

A single crystal was synthesized from KOsO<sub>4</sub> and Os in a sealed quartz tube with an appropriate amount of AgO for oxygen supply at 450 °C for 48 h. Energy-dispersive X-ray analysis in a scanning electron microscope indicated that the atomic ratio of K to Os is approximately equal to 0.5. Magnetic susceptibility was measured in a SQUID magnetometer (Quantum Design MPMS). Structural analyses were performed at 300, 200 and 100 K using a fresh crystal of 0.118 × 0.070 × 0.052 mm in a three-circle diffractometer equipped with a CCD area detector (Bruker SMART APEX) and a nitrogen-flow cooler. Oscillation photographs were taken at lower temperatures from 100 to 5 K using a curved imaging plate (MacScience DIP 320 V) and a helium closed-cycle refrigerator. Monochromatic Mo- $K\alpha$  radiation was used as the X-ray source. Data integration and global-cell refinements were performed with SAINT using data in the range  $2\theta = 4 - 107^\circ$ , and absorption correction was applied using SADABS [12]. Symmetry equivalent reflections were averaged to produce unique reflections ( $R_{\text{int}} = 0.051 - 0.055$ ). Structural parameters were refined by the full-matrix least-squares method using the TEXSAN program.

## 3. Results and discussion

Fig. 1 shows the temperature dependence of magnetic susceptibility measured in a magnetic field of 10 Oe using another single crystal obtained from the same batch as used in the X-ray experiments. A superconducting transition was observed below  $T_c = 9.6 \text{ K}$ , as previously reported [3]. The volume fraction estimated at 2 K in the zero-field cooling experiment is 144%, which means that nearly 100% volume of the crystal becomes superconductivity, taking into account the demagnetization correction.

The unit cell determined at 300, 200 and 100 K was  $a = 10.089(2)$ ,  $10.086(2)$  and  $10.083(2) \text{ \AA}$ , respectively. The systematic absence observed is consistent with space group  $Fd\bar{3}m$ . No additional reflections were observed over the temperature range 5–300 K, suggesting the absence of structural transitions, in contrast to the case of related  $\alpha$ -pyrochlore oxide Cd<sub>2</sub>Re<sub>2</sub>O<sub>7</sub>, for which two successive structural transitions of decreasing symmetry occur [13]. In

the first step to determine the crystal structure at 300 K, the positions of the Os and O atoms were fixed at the 16*c* and 48*f* sites, respectively, according to the direct method [14]. Then, we carefully tried to fix the position of the K atom using the Fourier method. Fig. 2 shows a difference Fourier map on the (1 1 0) plane around the 8*b* site, which was obtained by subtracting the structure factor calculated for the Os and O atoms from that observed at 300 K. Apparently, the K atom is found at the 8*b* (3/8, 3/8, 3/8) position, and both the 32*e* ( $x, x, x$ ) and 16*d* (1/2, 1/2, 1/2) positions are empty. The occupancy of the K atom is refined as 1.03(12), suggesting that there are no vacancies within the experimental error. Moreover, no evidence of water insertion such as reported for KNbWO<sub>6</sub> was detected in the present compound [10]. Essentially the same results were obtained at 200 and 100 K. The final  $R[F]$  ( $R_w[F^2]$ ) values were 0.028 (0.031), 0.027 (0.033) and 0.024 (0.029) for  $I > 3.0\sigma(I)$  at 300, 200 and 100 K, respectively. Therefore, the crystal structure of KOs<sub>2</sub>O<sub>6</sub> was determined to be the ideal  $\beta$ -pyrochlore structure. The refined structure parameters are given in Table 1.

Fig. 3 illustrates the crystal structure of KOs<sub>2</sub>O<sub>6</sub>. There are eight formula units per unit cell. The OsO<sub>6</sub> octahedra

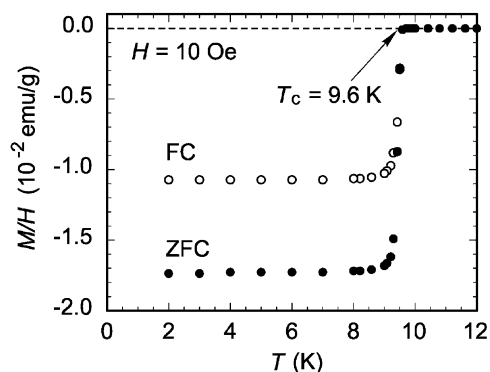


Fig. 1. Temperature dependence of magnetic susceptibility measured on a single crystal of KOs<sub>2</sub>O<sub>6</sub> in a magnetic field of 10 Oe. ZFC (●) and FC (○) indicate the zero-field cooling and the field cooling experiments, respectively.

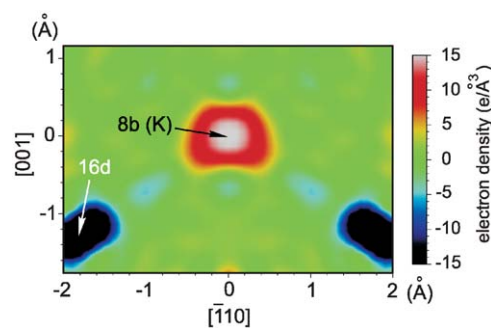


Fig. 2. Difference Fourier map at 300 K on the (1 1 0) plane around the 8*b* site (3/8, 3/8, 3/8) with the Os and O atoms subtracted. The 16*d* site (1/2, 1/2, 1/2) lies at the midpoint between neighboring 8*b* sites, and the 32*e* site ( $x, x, x$ ) at the midway between the 8*b* and 16*d* sites.

Table 1  
Atom coordinates and isotropic atomic displacement parameters for  $\text{KOs}_2\text{O}_6$  at 300, 200 and 100 K

Atom	Position	$x$	$y$	$z$	$100U_{\text{iso}}/(\text{\AA}^2)$
300.0(1) K	$a = 10.089(2) \text{\AA}$				
K	8b	0.375	0.375	0.375	7.35(8)
Os	16c	0	0	0	0.435(2)
O	48f	0.3145(8)	0.125	0.125	1.24(8)
200.0(1) K	$a = 10.086(2) \text{\AA}$				
K	8b	0.375	0.375	0.375	5.46(6)
Os	16c	0	0	0	0.353(2)
O	48f	0.3140(7)	0.125	0.125	1.23(7)
100.0(1) K	$a = 10.083(2) \text{\AA}$				
K	8b	0.375	0.375	0.375	3.89(4)
Os	16c	0	0	0	0.286(2)
O	48f	0.3155(6)	0.125	0.125	0.90(5)

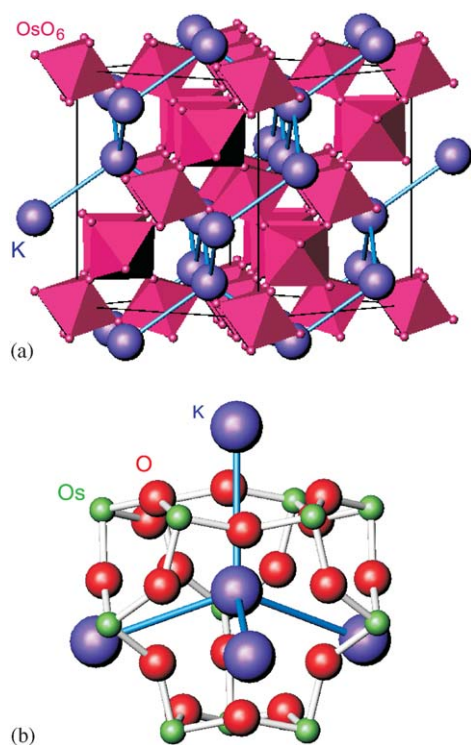


Fig. 3. Crystal structure of  $\beta$ -pyrochlore oxide  $\text{KOs}_2\text{O}_6$ . Corner-shared  $\text{OsO}_6$  octahedra form a three-dimensional network, and the K atoms at the 8b site are located in the center of the  $\text{Os}_{12}\text{O}_{18}$  cage as shown in (b). The K atoms hypothetically form a diamond sublattice with long K–K bonds through the four channels of the  $\text{Os}_{12}\text{O}_{18}$  cage along the  $\langle 111 \rangle$  direction.

share their corners to form a three-dimensional network. The atom coordinate  $x$  of O (48f) is a unique parameter that determines the distortion of an  $\text{OsO}_6$  octahedron. The deviation from the special value of  $x = 0.3125$  for the ideal octahedron leads to a trigonal distortion with an equal Os–O distance. The values of  $x = 0.3140$ – $0.3155$  observed for  $\text{KOs}_2\text{O}_6$  are much smaller than those for other

pyrochlore oxides with  $x = 0.32$ – $0.33$  [1]. This means that there is a small distortion of the octahedron, with internal O–Os–O angles of  $90.6$ – $91.2^\circ$  and  $88.8$ – $89.4^\circ$  and a large Os–O–Os angle of  $139.4$ – $140.2^\circ$  between neighboring octahedra, as listed in Table 2. The octahedral distortion seems to increase slightly at low temperature. The valence of Os is estimated to be  $+5.5$  from bond valence sum calculations using a bond valence parameter of 1.868 for  $\text{Os}^{5+}$  in the empirical formula and the Os–O bond distances obtained at 300 K [11,15]. This is in good agreement with the formal valence of  $+5.5$  expected from the purely ionic model.

Fig. 3(b) depicts another view of the crystal structure, showing that the K atom is located at the center of a cavity formed by an  $\text{Os}_{12}\text{O}_{18}$  cage with 6 nearest and 12 next-nearest oxygen neighbors. The cavity is open along four directions parallel to the  $\langle 111 \rangle$  direction. Thus, it can be assumed that four ‘hypothetical’ K–K bonds pass through these channels. The sublattice of K atoms is the ideal diamond lattice, with a long K–K distance of  $4.4 \text{\AA}$ . The diameter of the bottleneck of the channel formed by six oxygen atoms is approximately  $2.4 \text{\AA}$  and is smaller than the size of the K ion (approx.  $3.0 \text{\AA}$ ).

The most important finding in the present structural analysis is an unusually large atomic displacement parameter (ADP)  $U_{\text{iso}}$  for the K atom, at approximately 17- (14-) and six- (four-)times greater than that for the Os and O atoms at 300 K (100 K), respectively. In previous structural analyses of  $\text{CsOs}_2\text{O}_6$  and  $\text{RbOs}_2\text{O}_6$ , it was found that the A cations also exhibit large ADPs at room temperature, with  $U_{\text{iso}} = 0.025 \text{\AA}^2$  for Cs and  $U_{\text{iso}} = 0.043 \text{\AA}^2$  for Rb [11]. However, the present value of  $U_{\text{iso}} = 0.074 \text{\AA}^2$  for K is much greater. It is apparent from Fig. 4 that the smaller the ionic radius of the A cations, the larger is  $U_{\text{iso}}$  in  $\text{AOs}_2\text{O}_6$ . Similarly, large  $U_{\text{iso}}$  values have been observed in defect pyrochlore oxides (e.g.  $U_{\text{iso}} = 0.070 \text{\AA}^2$  for Rb in  $\text{RbNbWO}_6$ ) [10], filled skutterudites (e.g.  $U_{\text{iso}} = 0.051 \text{\AA}^2$  for Nd in  $\text{NdOs}_4\text{Sb}_{12}$ ) [16] and clathrates (e.g.

Table 2  
Os–O distance, O–Os–O bond angles in the octahedron and Os–O–Os bond angles at 300, 200 and 100 K

T (K)	Os–O (Å)	O–Os–O (°)	Os–O–Os (°)
300	1.898(3)	90.8(3)/89.2(3)	139.9(4)
200	1.896(3)	90.6(3)/89.4(3)	140.2(4)
100	1.901(2)	91.2(2)/88.8(2)	139.4(3)

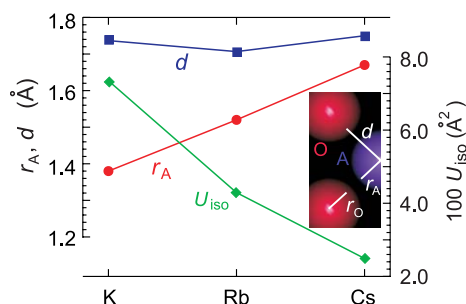


Fig. 4. Ionic radius  $r_A$  (Å) (●), the cavity radius of the cage  $d$  (Å) (■), and the isotropic atomic displacement parameter  $U_{\text{iso}}$  (Å<sup>2</sup>) (◆) for A = Cs, Rb and K in AOs<sub>2</sub>O<sub>6</sub> [11,18].

$U_{\text{iso}} = 0.033 \text{ Å}^2$  for Ba in Ba<sub>8</sub>Ga<sub>16</sub>Si<sub>30</sub>) [17]. In all the above compounds, the large ADPs are commonly interpreted as resulting from rattling of an atom in an oversized cage. It should be noted that the K atom in KOs<sub>2</sub>O<sub>6</sub> has the largest ADP value.

To gain an intuitive insight into the systematic changes in ADP observed for Cs, Rb and K in AOs<sub>2</sub>O<sub>6</sub>, we estimated the ‘size’ of the free space inside the Os<sub>12</sub>O<sub>18</sub> cage. A simple measure is the clearance  $d - r_A$ , where  $r_A$  is the ionic radius of A and  $d$  is a distance obtained by extracting the ionic radius of oxygen (1.4 Å) from the experimental A–O distance, as schematically shown in Fig. 4 [18]. It was found that  $d$  is almost insensitive to changes in A, implying that the Os–O framework is rigid. Thus, the clearance increases with decreasing  $r_A$  from Cs to K. It is obvious that  $U_{\text{iso}}$  increases with increasing clearance, which determines the space available for the A atom. Therefore, the K atom is the most weakly bound to the surrounding atoms and can rattle heavily.

Such a weakly bound atom in an oversized cage should induce dynamic instability. Kuneš et al. found an anharmonic potential for the A cation along the (111) direction in AOs<sub>2</sub>O<sub>6</sub> and larger anharmonicity for a smaller A cation [19]. In fact, the electron distribution of the K atom shown in the Fourier map of Fig. 2 is considerably elongated along the (111) direction, suggesting that there are tetrahedrally shaped lobes pointing to the four open channels of the Os<sub>12</sub>O<sub>18</sub> cage. It is difficult to explain this elongation at the 8b site within the harmonic treatment of thermal vibrations because of the high symmetry of the site in the expression of the anisotropic displacement parameters ( $U_{11} = U_{22} = U_{33}$  and  $U_{12} = U_{13} = U_{23} = 0$ ). This is clear evidence for the existence of an anharmonic

potential for the K atom at 300 K, which remains even at 100 K.

The large ADP observed can be ascribed to either dynamic atomic vibrations or static disorder. However, the previous experimental evidence that there is a large contribution from Einstein modes to the specific heat may exclude the latter possibility [20]. It is reasonable to treat the rattling species as an Einstein oscillator and the framework as a Debye solid. Provided that the two contributions are independent of each other, characteristic temperatures  $\Theta_E$  and  $\Theta_D$  can be estimated for the two modes from the temperature dependence of the mean-square displacement amplitude  $\langle u^2 \rangle = U_{\text{iso}}$ . Fig. 5 shows the temperature dependence of  $U_{\text{iso}}$  for K, Os and O atoms. The  $U_{\text{iso}}$  values for K and Os below 100 K were calculated from the intensity data of some selected reflections measured by the imaging plate. The mean-square displacement amplitude is given by  $\langle u^2 \rangle = u_0^2 + h^2 / (8\pi^2 m k_B \Theta_E) \coth(\Theta_E / 2T)$  for a harmonic oscillator, and  $\langle u^2 \rangle = 3h^2 / (4\pi^2 m k_B \Theta_D) T$  ( $T > \Theta_D$ ) for a Debye solid, where  $u_0$  is a temperature-independent parameter,  $h$  is Planck’s constant,  $k_B$  is the Boltzmann constant, and  $m$  is the atomic mass [21,22]. The Einstein temperature  $\Theta_E$  is estimated to be 86(2) K by fitting the data for K over the whole temperature range, and the Debye temperature  $\Theta_D$  is estimated to be 266(8) K using the average  $U_{\text{iso}}$  value and the average mass per atom for Os and O at 300 K. This  $\Theta_E$  value is close to the average value of two Einstein temperatures obtained from specific heat measurements [20]. The temperature-independent parameter was found to be very large:  $u_0 = 0.147(5) \text{ Å}$ . Generally, it is ascribed to certain disorder, but this may not be the case now. The large  $u_0$  value may indicate that the rattling of the K atom remains dynamic, even at low temperature, owing to the anharmonic potential with an almost flat bottom for the K atom [19].

Previous specific heat measurements detected an intensive peak centered at 7.5 K below  $T_c$ , which was not directly ascribed to superconductivity, but might be related to an unknown structural transition [23]. We carried out a preliminary structure analysis at 5 K. No evidence of a structural phase transition was detected. However, a further study is required to clarify this interesting possibility.

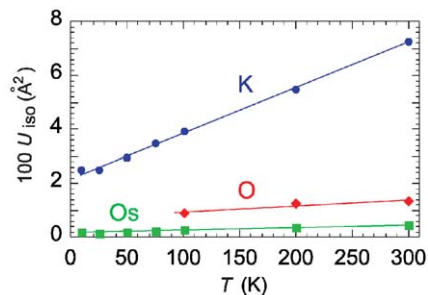


Fig. 5. Temperature dependence of the isotropic atomic displacement parameter  $U_{\text{iso}}$  for K (●), Os (■) and O (◆).

#### 4. Summary

In summary, the structure of  $\text{KO}_2\text{O}_6$  has been determined as the  $\beta$ -pyrochlore structure. The K atom is located at the  $8b$  site, not at the  $16d$  site as in conventional pyrochlore oxides, and thus at the center of the  $\text{Os}_{12}\text{O}_{18}$  cage. An anomalously large atomic displacement parameter was found for the K atom, which is because of rattling of the K atom in the oversized cage. It has been shown that the magnitude of rattling in  $\beta$ -pyrochlore oxides is determined by the clearance between the cavity of the cage and the cation: the greater the clearance from Cs to K, the greater is the rattling magnitude. In addition, it was found that the K atom vibrates with anharmonicity along the  $(1\ 1\ 1)$  direction to the open channels of the  $\text{Os}_{12}\text{O}_{18}$  cage.

#### Acknowledgments

We are grateful to Prof. Fukuyama for helpful discussions. This work was supported by a Grant-in-Aid for Scientific Research (B) (No. 16340101) provided by the Ministry of Education, Science, Sports, Culture and Technology, Japan.

#### References

- [1] M.A. Subramanian, G. Aravamudan, G.V. Subba Rao, *Prog. Solid State Chem.* 15 (1983) 5.
- [2] M. Hanawa, Y. Muraoka, T. Tayama, T. Sakakibara, J. Yamaura, Z. Hiroi, *Phys. Rev. Lett.* 87 (2001) 187001.
- [3] S. Yonezawa, Y. Muraoka, Y. Matsushita, Z. Hiroi, *J. Phys. Condens. Matter* 16 (2004) L9.
- [4] S. Yonezawa, Y. Muraoka, Y. Matsushita, Z. Hiroi, *J. Phys. Soc. Jpn.* 73 (2004) 819.
- [5] S. Yonezawa, Y. Muraoka, Z. Hiroi, *J. Phys. Soc. Jpn.* 73 (2004) 1655.
- [6] M. Brühwiler, S.M. Kazakov, N.D. Zhigadlo, J. Karpinski, B. Batlogg, *Phys. Rev. B* 70 (2004) 020503.
- [7] K. Arai, J. Kikuchi, K. Kodama, M. Takigawa, S. Yonezawa, Y. Muraoka, Z. Hiroi, *Phys. Rev. Lett.*, submitted for publication.
- [8] Z. Hiroi, S. Yonezawa, Y. Muraoka, *J. Phys. Soc. Jpn.* 73 (2004) 1651.
- [9] A. Koda, W. Higemoto, K. Ohishi, S.R. Saha, R. Kadono, S. Yonezawa, Y. Muraoka, Z. Hiroi, *J. Phys. Soc. Jpn.* 74 (2005) 1678.
- [10] P.W. Barnes, P.M. Woodward, Y. Lee, T. Vogt, J.A. Hriljac, *J. Am. Chem. Soc.* 125 (2003) 4572.
- [11] S. Yonezawa, T. Kakiuchi, H. Sawa, J. Yamaura, Y. Muraoka, F. Sakai, Z. Hiroi, *Solid State Sci.*, submitted for publication.
- [12] SAINT and SADABS, Programs for data collection and absorption correction, Bruker AXS Inc., Madison, WI, USA, 2000.
- [13] J. Yamaura, Z. Hiroi, *J. Phys. Soc. Jpn.* 71 (2002) 2598.
- [14] A. Altomare, M.C. Burla, M. Camalli, G. Cascarano, C. Giacovazzo, A. Guagliardi, A.G.G. Moliterni, G. Polidori, R. Spagna, *J. Appl. Cryst.* 32 (1999) 115.
- [15] N.E. Brese, M. O'Keeffe, *Acta Crystallogr. B* 47 (1991) 192.
- [16] C.B.H. Evers, W. Jeitschko, L. Boonk, D.J. Braun, T. Ebel, U.D. Scholz, *J. Alloys Compd.* 224 (1995) 184.
- [17] L. Qiu, I.P. Swainson, G.S. Nolas, M.A. White, *Phys. Rev. B* 70 (2004) 035208.
- [18] R.D. Shannon, *Acta Crystallogr. A* 32 (1976) 751.
- [19] J. Kuneš, T. Jeong, W.E. Pickett, *Phys. Rev. B* 70 (2004) 174510.
- [20] Z. Hiroi, personal communication.
- [21] B.C. Sales, B.C. Chakoumakos, D. Mandrus, *J. Solid State Chem.* 146 (1999) 528.
- [22] B.T.M. Willis, A.W. Pryor, *Thermal Vibrations in Crystallography*, Cambridge University Press, London, 1975.
- [23] Z. Hiroi, S. Yonezawa, T. Muramatsu, J. Yamaura, Y. Muraoka, *J. Phys. Soc. Jpn.* 74 (2005) 1682.